



**HAL**  
open science

## Holocene climatic changes in Greenland: Different deuterium excess signals at Greenland Ice Core Project (GRIP) and NorthGRIP

Valérie Masson-Delmotte, Amaelle Landais, M. Stievenard, O. Cattani, S. Falourd, Jean Jouzel, Sigfus J. Johnsen, Dorthe Dahl-Jensen, A. Sveinsbjornsdottir, J. W. C. White, et al.

### ► To cite this version:

Valérie Masson-Delmotte, Amaelle Landais, M. Stievenard, O. Cattani, S. Falourd, et al.. Holocene climatic changes in Greenland: Different deuterium excess signals at Greenland Ice Core Project (GRIP) and NorthGRIP. *Journal of Geophysical Research: Atmospheres*, 2005, 110 (D14102), 1 à 15 p. 10.1029/2004JD005575 . insu-00374873

**HAL Id: insu-00374873**

**<https://insu.hal.science/insu-00374873>**

Submitted on 14 Jan 2021

**HAL** is a multi-disciplinary open access archive for the deposit and dissemination of scientific research documents, whether they are published or not. The documents may come from teaching and research institutions in France or abroad, or from public or private research centers.

L'archive ouverte pluridisciplinaire **HAL**, est destinée au dépôt et à la diffusion de documents scientifiques de niveau recherche, publiés ou non, émanant des établissements d'enseignement et de recherche français ou étrangers, des laboratoires publics ou privés.

## Holocene climatic changes in Greenland: Different deuterium excess signals at Greenland Ice Core Project (GRIP) and NorthGRIP

V. Masson-Delmotte,<sup>1</sup> A. Landais,<sup>1</sup> M. Stievenard,<sup>1</sup> O. Cattani,<sup>1</sup> S. Falourd,<sup>1</sup> J. Jouzel,<sup>1</sup> S. J. Johnsen,<sup>2</sup> D. Dahl-Jensen,<sup>2</sup> A. Sveinbjornsdottir,<sup>3</sup> J. W. C. White,<sup>4</sup> T. Popp,<sup>4</sup> and H. Fischer<sup>5</sup>

Received 5 November 2004; revised 25 February 2005; accepted 12 April 2005; published 20 July 2005.

[1] Water stable isotope measurements ( $\delta D$  and  $\delta^{18}O$ ) have been conducted on the Holocene part of two deep Greenland ice cores (Greenland Ice Core Project (GRIP) and NorthGRIP), located  $\sim 320$  km apart. These combined measurements provide the first two continuous Greenland Holocene deuterium excess profiles ( $d = \delta D - 8\delta^{18}O$ ), a parameter strongly influenced by changes in moisture sources. We discuss here temporal and regional fluctuations of the deuterium excess within central to north Greenland, with a mean temporal resolution of  $\sim 4$  years. Although GRIP and NorthGRIP exhibit similar annual mean surface temperatures and  $\delta^{18}O$  levels, a significant offset of modern deuterium excess is observed between the two sites. We attribute this offset to a different mix of modern moisture sources, pointing to regional-scale differences in moisture advection toward Greenland. The common long-term deuterium excess Holocene increasing trend is probably related to the increased relative contribution of low-latitude moisture to Greenland snowfall, in response to the change in the Earth obliquity, as symmetrically observed in Antarctica. Three abrupt declines punctuate the GRIP excess record (8.2, 4.5, and 0.35 ka BP), suggesting associated reorganizations of the northern high latitudes hydrological cycle. The 8.2 ka BP event is characterized by (1) a rapid cooling followed by a progressive warming and (2) a deuterium excess cooling restricted to GRIP, therefore totally different from rapid events during glacial times. By contrast, the NorthGRIP deuterium excess record is more stable. We propose that a slightly larger proportion of moisture supplied by local storm tracks to GRIP induces an isotopic compensation mechanism between simultaneous site and source temperature coolings, resulting in a rather temperature-insensitive  $\delta^{18}O$  profile, together with well-marked deuterium excess amplitudes. NorthGRIP  $\delta^{18}O$  seems less biased by isotopic processes and should provide a more reliable past temperature record.

**Citation:** Masson-Delmotte, V., et al. (2005), Holocene climatic changes in Greenland: Different deuterium excess signals at Greenland Ice Core Project (GRIP) and NorthGRIP, *J. Geophys. Res.*, 110, D14102, doi:10.1029/2004JD005575.

### 1. Introduction

[2] In the context of the ongoing climate change [Houghton, 2001], detailed and quantitative reconstructions of the Holocene climate are necessary to provide fruitful insights on warm period climate variability. The sensitivity of climate to obliquity and precession fluctuations involves

significant changes in the meridional temperature gradients [Liu *et al.*, 2003; Vimeux *et al.*, 2001] and in the seasonal changes of oceanic and atmospheric circulation, already well documented in the tropics [Braconnot *et al.*, 2000] and midlatitudes [Masson *et al.*, 1999]. The early Holocene is probably recording complex reorganizations in response to the decay of the continental ice sheets and the large solar radiation forcing. In the North Atlantic, a rapid climatic change has taken place during the last episode of the Laurentide ice sheet collapse (8.2 kaBP) [Alley *et al.*, 1997; Barber *et al.*, 1999; Grafenstein *et al.*, 1998]. The improved knowledge of centennial-scale climate variability during the Holocene in the north Atlantic area provided by high-resolution records from marine sediments [Marchal *et al.*, 2002; Rimbu *et al.*, 2003], speleothems [McDermott *et al.*, 2001] and ice cores [Johnsen *et al.*, 2001; O'Brien *et al.*, 1995] enables us to explore the possibility of recurrent millennial-scale oscillations [Bianchi and Cave, 1999; Bond *et al.*, 1997].

<sup>1</sup>Institut Pierre-Simon Laplace/Commissariat à l'Énergie Atomique, CNRS Laboratoire des Sciences du Climat et de l'Environnement, Gif-sur-Yvette, France.

<sup>2</sup>Niels Bohr Institute, University of Copenhagen, Copenhagen, Denmark.

<sup>3</sup>Science Institute, University of Iceland, Reykjavik, Iceland.

<sup>4</sup>Geological Sciences Department, University of Colorado, Boulder, Colorado, USA.

<sup>5</sup>Alfred Wegener Institute for Polar and Marine Research, Bremerhaven, Germany.

[3] Sampling the “cold end” of the atmospheric hydrological cycle in each hemisphere, polar ice cores offer an excellent archive of past precipitation and of their stable isotopic composition. This parameter has long been used to reconstruct past local temperatures [Dansgaard, 1964; Jouzel et al., 1997, 2003]. The stable isotopic composition of an atmospheric water mass is acquired during the evaporation at the ocean surface and depends on the evaporation conditions (seawater isotopic composition, sea surface temperature, and kinetics of the evaporation driven by the sea surface temperature, relative humidity of the air mass above, and surface wind speed) [Cappa et al., 2003; Merlivat and Jouzel, 1979]. During the progressive cooling of the air masses along their path to polar ice sheets, they undergo an isotopic distillation with the preferential loss of heavy isotopes into the rain and snowfalls, controlled by the condensation temperature. As a result of the progressive air mass distillation, a linear relationship is observed between modern precipitation isotopic composition and modern surface temperature [Craig and Gordon, 1965; Fischer et al., 1995; Johnsen et al., 1989; Kavanaugh and Cuffey, 2003; Rozanski et al., 1993] with a slope of 0.67‰ per °C at northern high latitudes. Whether this relationship holds true for local temperature changes in time depends on the stability of the moisture source evaporation conditions, on the distillation history and on the relative changes in condensation versus surface temperature. During glacial periods, alternative paleothermometry methods have shown that this assumption does not hold for Greenland, neither at the glacial-interglacial timescale (borehole temperature inversion [Dahl-Jensen et al., 1998]), nor during rapid events (firn air isotope thermal diffusion, [see, e.g., Landais et al., 2004a, 2004b; Severinghaus and Brook, 1999; Severinghaus et al., 1998]). Last Glacial Maximum climate simulations conducted with atmospheric general circulation models [Fawcett et al., 1995; Krinner, 1997; Werner et al., 2000] showed that very dry winter conditions prevailed in central Greenland during glacial times, resulting in dramatic biases in the quantitative isotopic interpretation. Recent studies have also suggested that changes in the northern hemisphere stationary waves (resulting in apparent changes in the North Atlantic Oscillation index) may significantly influence Greenland accumulation and isotopic composition [Appenzeller et al., 1998; Barlow et al., 1993; Bromwich et al., 1999; Vinther et al., 2003]. Changes in atmospheric circulation, simulated for instance in response to the Maunder minimum solar activity forcing [Shindell et al., 2001] and associated isotopic processes (changes in snowfall seasonality, changes in moisture source), may therefore bias Greenland  $\delta^{18}\text{O}$ –temperature relationships. A correct quantitative temperature estimation using Greenland ice  $\delta^{18}\text{O}$  requires additional constraints on past atmospheric circulation and hydrological cycle changes.

[4] The combined measurements of both  $\delta\text{D}$  and  $\delta^{18}\text{O}$  of precipitation supply complementary information on evaporation conditions, therefore on past hydrological cycle changes. The kinetic fractionation occurring during evaporation at the ocean surface (the “moisture source”) and during snow crystal formation [Jouzel and Merlivat, 1984] have different relative imprints on  $\delta^{18}\text{O}$  and  $\delta\text{D}$  of the initial water vapor, leading to a specific signal in the deuterium excess defined as:  $d = \delta\text{D} - 8\delta^{18}\text{O}$  [Dansgaard, 1964]. Here

the slope of 8 is governed by the equilibrium fractionation coefficients for the hydrogen and oxygen isotopes. Changes in the kinetics of evaporation, different temperature dependence of the equilibrium fractionation coefficients for  $\delta\text{D}$  and  $\delta^{18}\text{O}$  and an additional kinetic fractionation during the condensation of supersaturated vapor on ice crystals [Jouzel and Merlivat, 1984] induce deviations from this 8 slope and therefore deuterium excess fluctuations.

[5] Only a few studies have been dedicated to deuterium excess fluctuations in Greenland snow and ice, highlighting the role of evaporation conditions and specifically moisture source temperature. We know that the mean modern seasonal cycle of the deuterium excess in central Greenland is shifted by 2–3 months with respect to local temperature and  $\delta^{18}\text{O}$  [Hoffmann et al., 1998; Johnsen et al., 1989], reflecting the thermal inertia of the surface ocean temperature. A deuterium excess record covering the last millennium from two ice cores at Summit (location of Greenland Ice Core Project (GRIP) on Figure 1a) showed a marked moisture source cooling during the Little Ice Age [Hoffmann et al., 2001]; the authors suggested that central Greenland actually underwent a Little Ice Age cooling but it may have been masked in the  $\delta^{18}\text{O}$  record because of site and source temperature compensating effects. Holocene-long deuterium excess fluctuations have so far only been analyzed in Antarctic ice cores as reviewed by [Masson-Delmotte et al., 2004; Vimeux et al., 2001], showing a large site to site dispersion as well as a common Holocene increasing trend. It was proposed that this increase is the result of different annual mean insolation changes at low and high latitudes, in response to the Holocene change in obliquity (Figure 1c). A progressive cooling of high latitudes and a warming of low latitudes should result in a more efficient transport of moisture from warmer low-latitude sources to Antarctica. If this hypothesis is correct, and moisture sources are located at equivalent latitudes in the northern hemisphere, then similar trends should be also detected in Greenland, because obliquity fluctuations modify simultaneously and symmetrically the annual mean insolation in the two hemispheres.

[6] Here we present the first two Greenland deuterium excess records covering the Holocene, measured on two deep ice cores at a bag sample (55 cm) resolution, therefore with a mean temporal resolution of  $\sim 4$  years. We compare the isotopic records of GRIP [Dansgaard et al., 1993] and NorthGRIP [Dahl-Jensen et al., 1997; Johnsen et al., 2001], with respect to (1) modern isotopic ratios; (2) Holocene trends and changes in semidecadal variability; and (3) Holocene rapid events, focusing on the deuterium excess signal and the moisture sources. Measurements were conducted on the same samples in Copenhagen for  $\delta^{18}\text{O}$  (analytical precision of  $\pm 0.05\text{‰}$ ) and in Saclay for  $\delta\text{D}$  (analytical precision of  $\pm 0.5\text{‰}$ ), resulting in an overall precision of  $\pm 0.7\text{‰}$  for the deuterium excess in each sample. The common age scale is established from GRIP layer counting and stratigraphic markers including volcanic horizons [Johnsen et al., 2001] and the maximum relative error between GRIP and NorthGRIP age scales is estimated to be  $\sim 20$  years.

## 2. Modern Isotopic Levels

[7] The NorthGRIP drilling site (75.10°N and 42.32°W) is located  $\sim 320$  km to the north of the Greenland summit

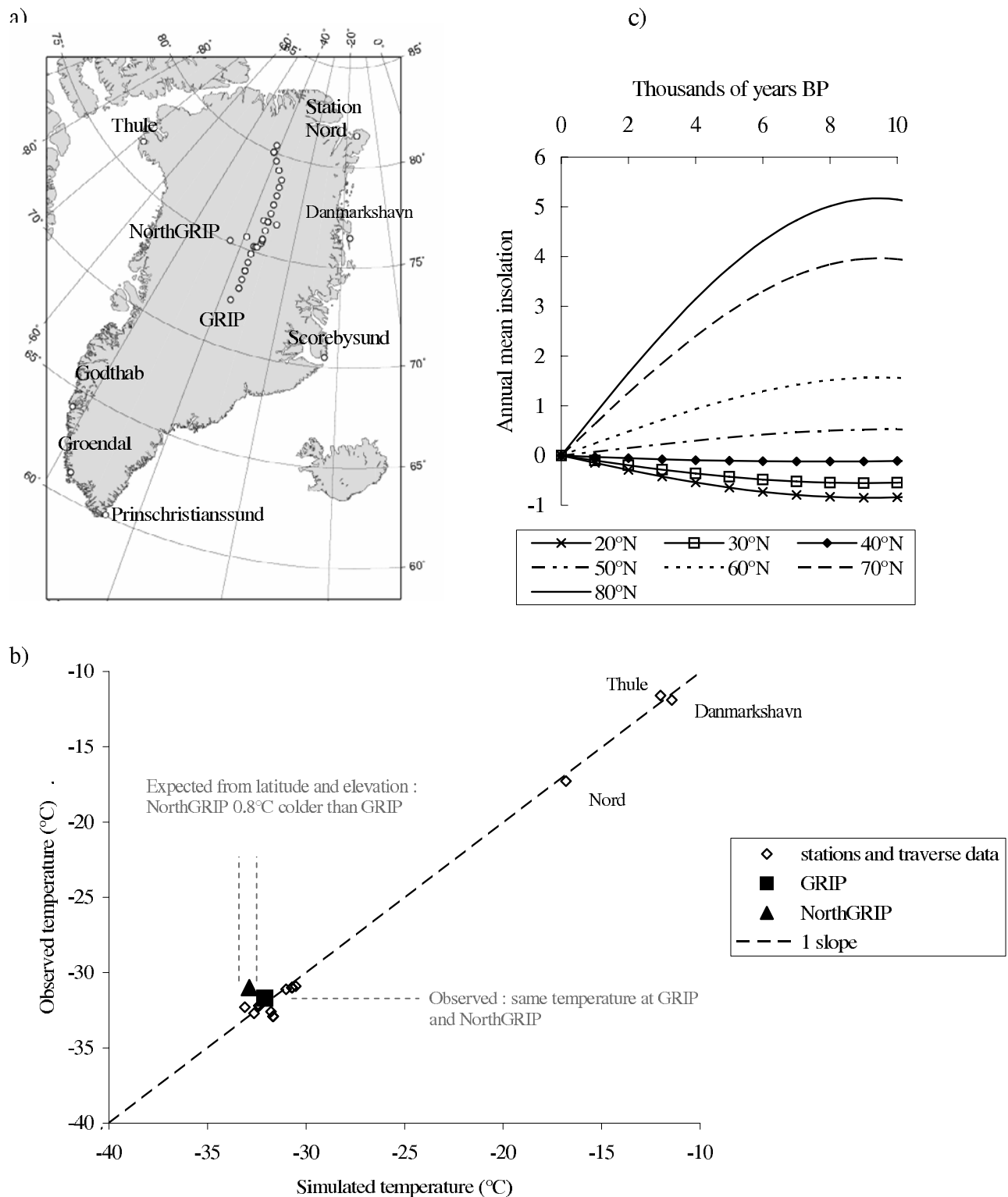


**Figure 1.** (a) Map of Greenland showing the location of GRIP and NorthGRIP deep drilling sites as well as the North Greenland traverse stable isotope sampling sites and the coastal IAEA stations. (b) Surface temperature: observed annual mean surface temperature (station and traverse data from Figure 1a) versus estimated annual mean surface temperature using local elevation and latitude (with the observed slopes of  $-7.9^{\circ}\text{C}$  per 1000 m elevation and  $-1.01^{\circ}\text{C}$  per  $^{\circ}\text{N}$  latitude). (c) Holocene changes in annual mean insolation at various latitudes, expressed in anomalies with respect to modern values, in  $\text{W}/\text{m}^2$ .

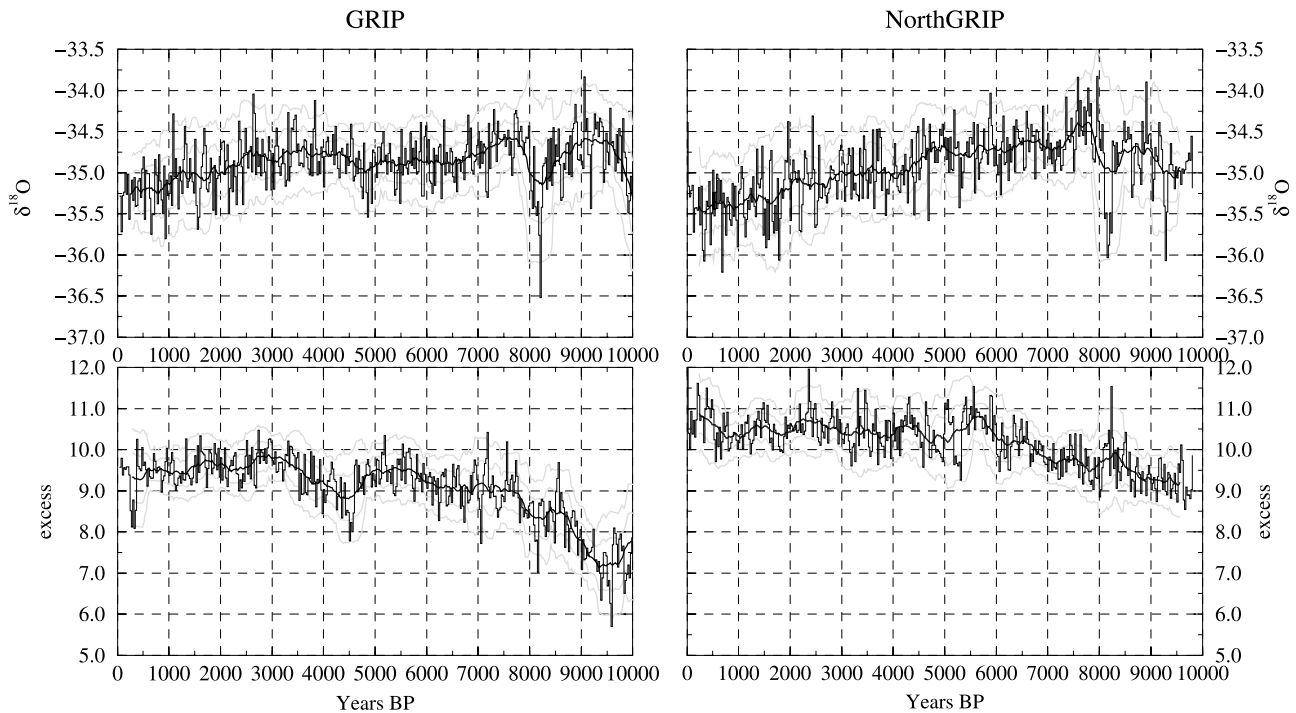


**Figure 2a.** Twenty-five year resampled isotopic fluctuations at (left) GRIP and (right) NorthGRIP (solid steps) and 20 point (500 year) running averages (bold solid line) and standard deviation above/below the running average ( $\pm 1\sigma$  and  $2\sigma$ , shaded lines). The upper part of the NorthGRIP record is obtained by stacking two shallow cores (S1 and S2) with the upper part of the deep ice core. (top) The  $\delta^{18}\text{O}$  (‰) and (bottom) deuterium excess (‰). The running standard deviations can be used to identify rapid events.

where the GRIP ice core was drilled ( $72.35^{\circ}\text{N}$ ,  $38.30^{\circ}\text{W}$ ) (Figures 1a and 1b). The two sites differ by their surface elevation (2917 m at NorthGRIP versus 3200 m at summit), mean modern accumulation (19 versus 23 cm of water equivalent per year) and have similar mean modern surface temperatures ( $-31.6$  and  $-31.7^{\circ}\text{C}$ ). The modern NorthGRIP  $\delta^{18}\text{O}$  is slightly more depleted than at GRIP ( $-35.5$  versus  $-35.2\text{‰}$ ), and its deuterium excess is significantly higher than at GRIP (10.5 versus 9.5‰) (Figures 2a and 2b).

[8] The two sites are located in slightly different contexts which may lead to different meteorological conditions. Most atmospheric general circulation models do not have enough spatial resolution to capture the different moisture origins and atmospheric circulations for such nearby sites in central Greenland. These models suggest a dominant moisture origin of central Greenland precipitation provided by the Atlantic ocean and polar seas (60% of the total modern precipitation in modern conditions) [Werner *et al.*, 2001], with a strong seasonal variability including a summer contribution from North America and the Pacific Ocean. We can call upon the following three processes to explain the different isotopic levels at GRIP and NorthGRIP.

[9] 1. The seasonality of modern precipitation is different. Field observations suggest a more regular year-round snow deposition at NorthGRIP than at GRIP, where large cyclones are associated with intense snow fall. However, such a bias should more strongly affect the  $\delta^{18}\text{O}$  level than the excess level, because of its much larger seasonal amplitude.

[10] 2. NorthGRIP is located downstream of GRIP on a common air mass distillation trajectory (see Appendix A and Figure 3). This is consistent with a reduced local NorthGRIP accumulation, more depleted  $\delta^{18}\text{O}$  levels and slightly higher excess levels. Different vertical temperature profiles at the two sites may indeed result in colder condensation temperatures at NorthGRIP than GRIP, although not reflected in surface temperatures.

[11] 3. Moisture sources are slightly different. Isotopic modeling (see Appendix A and Figure 3) suggests that a 1–2°C weighted mean warmer moisture source for NorthGRIP compared to GRIP would be compatible with the observed isotopic levels. The probability that NorthGRIP and GRIP have slightly different moisture origins nowadays is also compatible with observations from coastal GNIP stations and isotope data derived at the Institute for Environmental Physics, University of Heidelberg, on ice cores and snow pits collected along the AWI North Greenland traverse [Fischer *et al.*, 1998]. The  $\delta^{18}\text{O}$  of modern surface snow obtained from shallow cores in north western Greenland shows a common first-order relationship with surface temperature (either directly measured or extrapolated from direct measurements using a linear dependency on both elevation and latitude) (Figure 3). The apparent  $\delta^{18}\text{O}$ –site temperature slope (see caption of Figure 3) is  $0.72\text{‰}/^{\circ}\text{C}$  ( $r^2 = 0.96$ ,  $n = 50$ ), consistent with other data sets [Johnsen *et al.*, 1989]. Between  $75^{\circ}$  and  $77^{\circ}\text{N}$ , particularly low  $\delta^{18}\text{O}$  and high excess also possibly reflect the larger



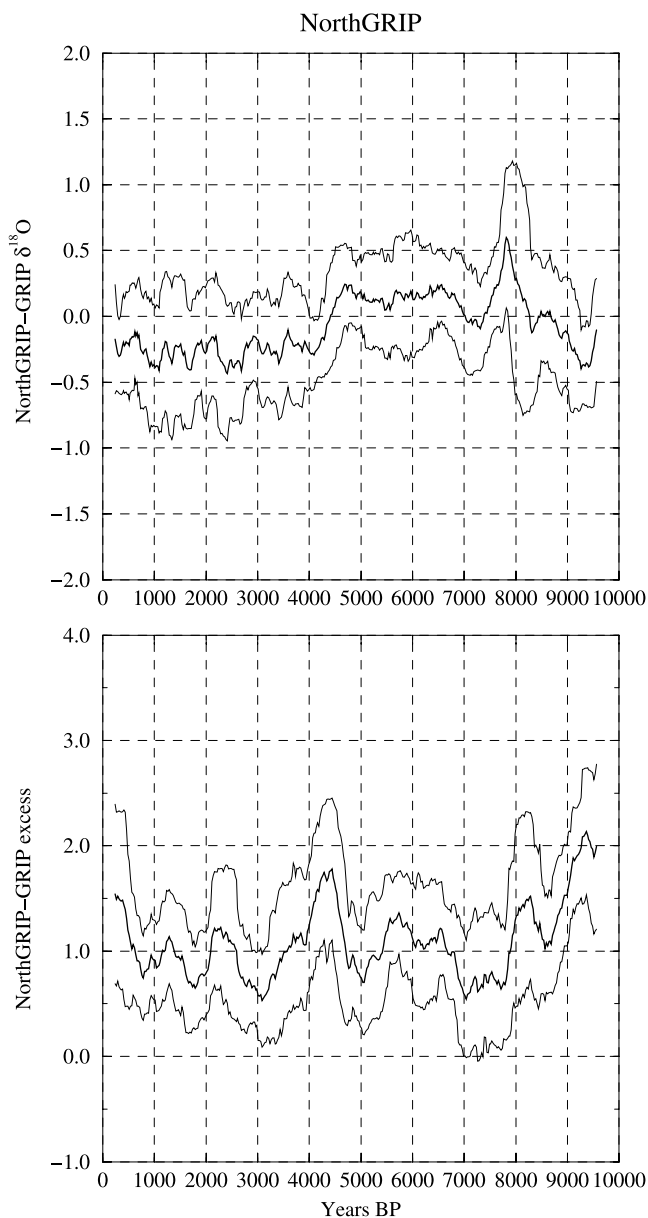


**Figure 2b.** Gradient between NorthGRIP and GRIP (top)  $\delta^{18}\text{O}$  (‰) and (bottom) deuterium excess (‰). Running averages over 20 points (500 years) and associated running standard deviation ( $\pm 1\sigma$ ) are shown.

contribution of remote warm moisture sources in northern Greenland.

[12] In summary, NorthGRIP and GRIP modern isotopic levels can be explained by two processes: First, NorthGRIP is located downstream on a common air mass distillation passing through GRIP; second, a slightly larger relative contribution of moisture evaporated with higher fractionation (e.g., from warmer oceanic areas), and transported at higher atmospheric levels toward NorthGRIP. The isotopic inversion performed on mean modern levels clearly rules out (Figure 3 and Appendix A) a similar moisture source for the two sites, even though similar surface temperatures are observed (Figure 1b): it suggests that the mean modern isotopic levels of the two sites are compatible with a  $0.6^\circ\text{C}$

lower condensation temperature at NorthGRIP (which is not observed at the surface) and a  $1.5^\circ\text{C}$  warmer source temperature for NorthGRIP, relative to GRIP.

[13] We propose that these slightly different moisture sources for GRIP and NorthGRIP result from slightly different atmospheric transport processes. At GRIP, a higher proportion of precipitation is delivered by cyclonic activity, bringing water vapor essentially from the regions of cyclogenesis (e.g., polar front). At northward latitudes such as NorthGRIP, the amount of precipitation related to cyclones diminishes, and a somewhat larger proportion of the moisture reflects the higher-level water vapor transport, coming from source regions further south. This hypothesis is supported by precipitation estimates over Greenland, showing the effect of the ice sheet dome in blocking the northward penetration of cyclones [Bromwich *et al.*, 1998, 1999].

### 3. Holocene Trends

[14] We have extracted the long-term isotopic trends using a 500 year running average performed on data sampled at a 25 year time step (Figure 2a). The GRIP  $\delta^{18}\text{O}$  record shows a small early Holocene optimum about 8000 years ( $+0.6\text{‰}$  higher than modern levels) ago followed by a small relative minimum about 6000 years ago, a second optimum about 4000 years ago ( $+0.5\text{‰}$ ), and a slow decrease interpreted as a cooling to modern levels. By contrast, NorthGRIP  $\delta^{18}\text{O}$  reveals a more pronounced early Holocene optimum ( $+0.8\text{‰}$ ), followed by a plateau until about 4500 years ago, when the same decrease toward modern levels starts.

[15] The GRIP excess record shows a first  $2\text{‰}$  increase from 9500 years to 8000 years, and a  $0.5\text{‰}$  slower increase until about 5000 years ago, interrupted by a prolonged drop about 4500 years ago, and a second large increase toward a  $0.5\text{‰}$  excess maximum about 3000 years ago; after this relative maximum, the GRIP excess decreases toward modern levels. NorthGRIP excess exhibits the same long-term behavior, although with only half of the amplitude: a  $1\text{‰}$  increase from the early Holocene toward a first maximum about 6000 years ago, then a small plateau and a second maximum ( $+0.3\text{‰}$ ) about 3000 years ago and the decrease toward modern levels.

[16] Such an early Holocene increasing excess trend has already been observed for central Antarctic ice cores [Vimeux *et al.*, 2001] and could be related to the decrease in the Earth's obliquity [Berger, 1978]. Changes in obliquity control changes in annual mean insolation, and probably annual mean ocean surface temperatures [Liu *et al.*, 2003], thereby playing a large role in the meridional atmospheric transport, and the relative contribution of low versus high latitudes on polar moisture origin. This change could partly account for the deuterium excess increase during the first half of the Holocene. Sea surface temperature reconstructions from the north Atlantic and Polar Seas deep sea cores drilled at latitudes from  $45^\circ\text{N}$  to  $75^\circ\text{N}$  [Andersen *et al.*, 2004; Marchal *et al.*, 2002; Rimbu *et al.*, 2003] show cooling ranges of  $1.5$  to  $4^\circ\text{C}$  over the last 10 000 years. Recent records obtained from trace elements in tropical Atlantic sediment cores [e.g., Rühlemann *et al.*, 1999] suggest an increasing trend by typically  $1^\circ\text{C}$  in 10,000 years. Warmer

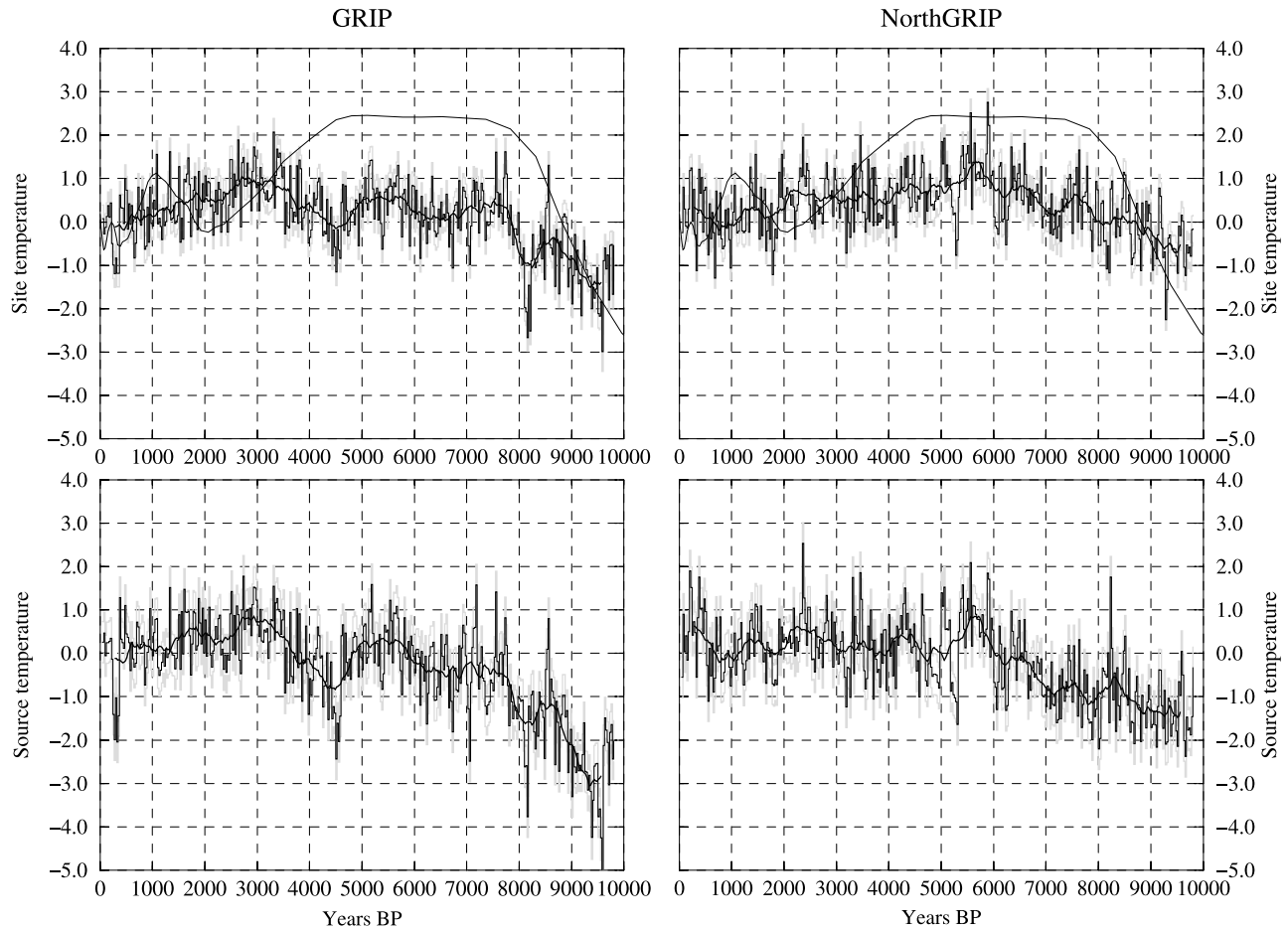


**Figure 2c.** GRIP temperature derived from the borehole temperature profile [Dahl-Jensen *et al.*, 1998] (solid line). (left) GRIP and (right) NorthGRIP (top) site and (bottom) source temperatures derived from GRIP and NorthGRIP  $\delta^{18}\text{O}$  and deuterium excess corrected for seawater  $\delta^{18}\text{O}$  (until 6000 BP) and inverted using equations (A3) and (A4). Shaded lines show an estimate of the uncertainties due to the tuning of the isotopic model and the analytical precision.

subtropics (thereby higher evaporation), cooler high latitudes (and reduced high-altitude evaporation) are consistent with the observed warming of central Greenland moisture source.

[17] The  $\delta^{18}\text{O}$  gradient between NorthGRIP and GRIP (Figure 2b) shows that there are two situations: In the early and late Holocene, NorthGRIP  $\delta^{18}\text{O}$  is more depleted than at GRIP; however, from about 8500 to 4500 years ago, the situation is reversed, with NorthGRIP  $\delta^{18}\text{O}$  on the contrary higher than in GRIP. The Holocene-long decrease of annual mean insolation (Figure 1c) is larger at higher latitudes (decrease of  $\sim 3.2 \text{ W/m}^2$  at  $60^\circ\text{N}$  and of  $\sim 4.2 \text{ W/m}^2$  at  $70^\circ\text{N}$ ) and is expected to be slightly larger at NorthGRIP than at GRIP (typically by  $0.5 \text{ W/m}^2$ ). At lower latitudes (typically south of  $\sim 43^\circ\text{N}$  here), the annual mean insolation shows a Holocene long increase with larger amplitudes at lower latitudes (increase of  $\sim 1 \text{ W/m}^2$  at  $20^\circ\text{N}$ , almost no change at  $40^\circ\text{N}$ ). Considerations about local summer insolation also suggest that the early Holocene optimum should be more marked northward: for instance, the June–July–August insolation gradient between  $72^\circ$  and  $75^\circ\text{N}$  is enhanced by 27% at 10,000 years BP compared to the modern situation. Together with this orbital forcing,

changes in sea ice cover and heat advection could indeed explain that warmer conditions typical of the early to mid-Holocene are associated with a decreased latitudinal temperature gradient in Greenland.

[18] This  $\delta^{18}\text{O}$  gradient cannot be explained by changes in source conditions because the deuterium excess of NorthGRIP is systematically larger than the deuterium excess of GRIP (Figure 2b), with a maximum deuterium excess gradient found during the early Holocene.

[19] We can quantify the relative influence of changes in site and source temperature using simple isotopic modeling (Appendix A and Figure 2c). Such a crude inversion suggests a  $1.5$  to  $2^\circ\text{C}$  warming from 10 to 8000 years BP in GRIP and NorthGRIP, and a  $0.5^\circ\text{C}$  local Holocene optimum from  $\sim 8000$  to 6500 years ago. The GRIP source temperature shows a  $3^\circ\text{C}$  temperature increase until 6000 years ago, still larger than the  $\sim 1.5^\circ\text{C}$  similar source temperature change at NorthGRIP (Figure 2c). Altogether, both deuterium excess and inferred moisture source temperature change estimates suggest large reorganizations in GRIP moisture advection compared to a more stable situation for NorthGRIP moisture origin. The significant deuterium excess trends during the early Holocene therefore

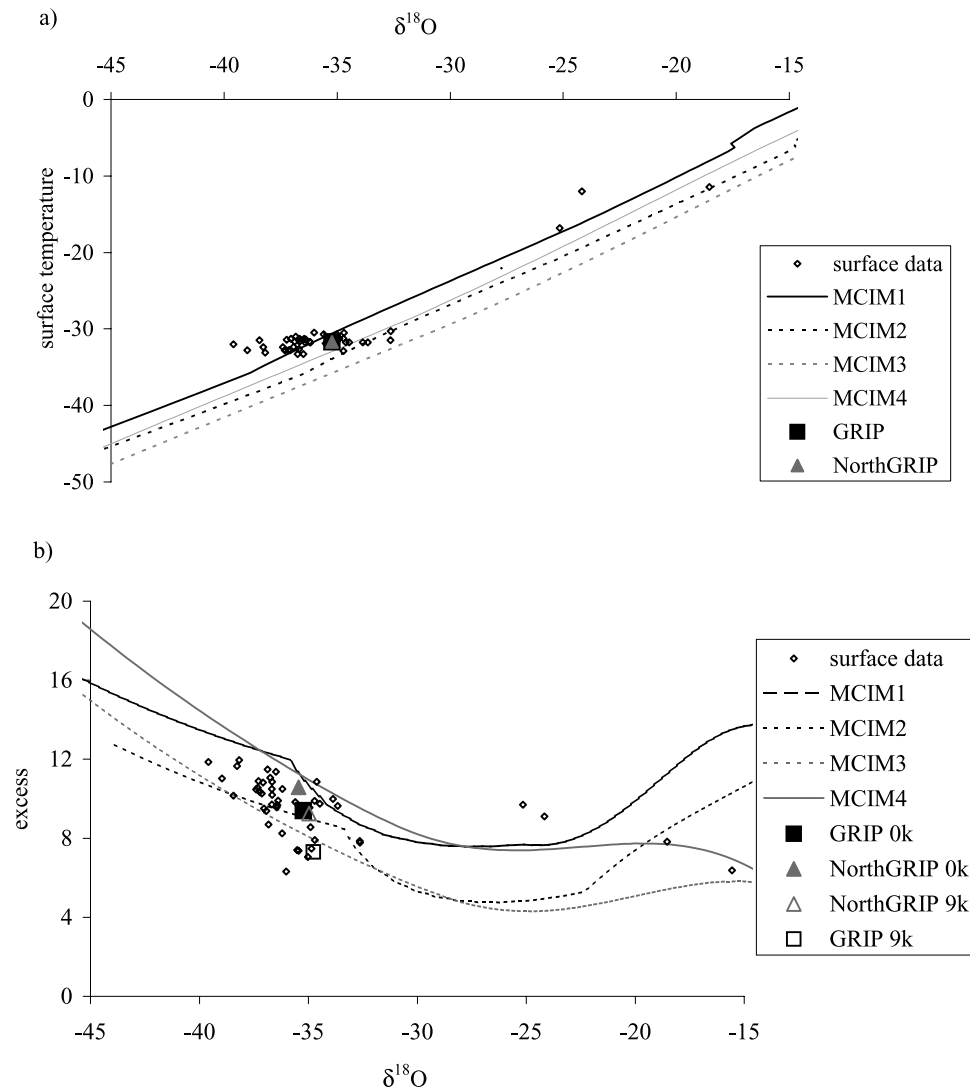


**Figure 3.** (a) The  $\delta^{18}\text{O}$  (x axis) versus local surface temperature (y axis). Surface temperatures are either directly available or are estimated from a linear regression on site latitude and elevation, fitted to the 19 direct temperature measurements available among the Greenland sites described in Figure 1a (with slopes of  $7.9^\circ\text{C}$  per 1000 m elevation and a slope of  $1.0^\circ\text{C}$  per degree latitude); long-term mean annual  $\delta^{18}\text{O}$  is estimated from IAEA stations along the duration of monitoring and over the last 50 years from traverse pits (squares) and from GRIP and NorthGRIP (triangles) ice cores. Simulations performed with the MCIM isotopic model with source temperatures of  $15^\circ\text{C}$  (dashed line) and  $20^\circ\text{C}$  (solid line) are also displayed, with two versions of the MCIM (Merlivat coefficients, MCIM1 and 2, and Cappa coefficients, MCIM3 and 4). The model-data disagreement for coastal stations might result from large contribution of local moisture supply with colder source temperatures. (b) Same as Figure 3a but for observed and simulated deuterium excess as a function of  $\delta^{18}\text{O}$ . See color version of this figure at back of this issue.

suggest that  $\delta^{18}\text{O}$  trends might be significantly biased by source temperature effects, which, when taken into account, lead to a better consistency with the borehole derived surface temperature both in terms of timing and amplitude of the mid-Holocene optimum:  $\sim 0.5$  to  $1^\circ\text{C}$  from the isotopes, to compare to a maximum of  $2.4^\circ\text{C}$  from the borehole profile, with uncertainties on the timing of peak warmth depending of the borehole inversion methods [Cuffey *et al.*, 1995; Dahl-Jensen *et al.*, 1998]. The borehole estimate is consistent with other constraints from the Arctic [Fisher *et al.*, 1995]. New insights on regional temperature changes will

certainly arise from the inversion of NorthGRIP borehole temperature profile.

[20] Another bias in  $\delta^{18}\text{O}$  records from deep ice cores is the intermittency of the snowfall. Drastic changes in snowfall seasonality have been suggested to control the apparent glacial-Holocene discrepancy between borehole and gas fractionation thermometry compared to isotopic levels in GRIP ice cores. This hypothesis has been verified using glacial climate atmospheric general circulation simulations. Seasonality changes during the Holocene are expected to take place in response to changes in the insolation seasonal



cycle because of precession (with a 10% decrease of summer insolation from 10 000 years ago to nowadays and an associated 10% decrease in the amplitude of the seasonal cycle of local insolation). Holocene-long simulations performed with an intermediate complexity climate model suggest a 3°C temperature cooling from 9000 years ago to present, mainly in summer, larger in northern high latitudes, together with about 10% changes in precipitation seasonality which should have reinforced the temperature signal in Greenland  $\delta^{18}\text{O}$  [Renssen *et al.*, 2005].

[21] Changes in northern hemisphere winter stationary waves have been suggested to respond to precession during mid-Holocene [Rimbu *et al.*, 2003], and to natural forcings [Shindell *et al.*, 2001]. Although high-resolution isotopic measurement and back diffusion studies can enable the extraction of the winter  $\delta^{18}\text{O}$  signal [Vinther *et al.*, 2003], it is not possible to reconstruct the seasonality of accumulation. From considerations of the modern NAO imprint on Greenland climate, a mean mid-Holocene change inducing a positive NAO atmospheric pattern during winter [Rimbu *et al.*, 2003] would result in warmer temperatures south of Greenland (possibly all year round because of ocean inertia) and an increase in winter snowfall, in addition to warmer conditions in northwestern Europe and cooler conditions in southern Europe [Masson *et al.*, 1999]. Ignoring source effects (because the deuterium excess change between mid-Holocene and recent times is weak), an increase in the relative contribution of winter snowfall during warmer annual mean conditions is expected to result in a “cold bias” and an underestimation of local temperature changes from the annual mean  $\delta^{18}\text{O}$  signal in central Greenland ice cores. This hypothesis could be tested using different coupled ocean-atmosphere simulations of mid-Holocene response to orbital forcing.

#### 4. Holocene Variability

[22] There is no periodic millennial-scale component in any of the GRIP and NorthGRIP Holocene signals but a succession of aperiodic fluctuations. NorthGRIP and GRIP  $\delta^{18}\text{O}$  profiles show two “bifurcation” points where they have distinct millennial-scale behaviors (Figure 2a): first, around 8 to 7000 years BP (much larger positive anomaly for NorthGRIP), and second, from 5 to 4000 years BP (much larger decrease at NorthGRIP than GRIP). These two time periods correspond to large reorganizations in the northern hemisphere climate system.

[23] In order to identify rapid events we have plotted the running average plus or minus one or two running standard deviations with a 500 year time step (Figure 2a). A variety of rapid positive or negative excursions can be identified for each record (respectively 6, 7, 6, and 7 positive rapid events for GRIP  $\delta^{18}\text{O}$ , NorthGRIP  $\delta^{18}\text{O}$ , GRIP excess and NorthGRIP excess; and 10, 9, 9 and 3 negative rapid events). It is particularly remarkable that sharp rapid decreases of GRIP  $\delta^{18}\text{O}$  and excess and NorthGRIP  $\delta^{18}\text{O}$  occur not only about 8200 years ago, but also in the previous and following millennia. Some of these events are larger than others with a longer duration and will be discussed in more detailed hereafter.

[24] The 8.2 ka BP event is the last abrupt change in the thermohaline circulation, because of abrupt meltwater

inflow from the Laurentide ice sheet and detected in Greenland and Europe [Grafenstein *et al.*, 1998; McDermott *et al.*, 2001]. The 4.5 ka BP event is documented in some north Atlantic SST and continental [Lauritzen, 2003] records and takes place after major changes in the tropics (end of the humid African period) [Gasse and Van Campo, 1994]. These two time periods correspond to different  $\delta^{18}\text{O}$  fluctuations at GRIP and NorthGRIP. The small isotopic differences between GRIP and NorthGRIP may correspond to subtle changes in precipitation seasonality, atmospheric vertical structure (condensation versus surface temperature), and moisture origin. We have no available data to assess the first two points, but the deuterium excess data should help to constrain past changes in moisture origin.

[25] In addition to the Little Ice Age (LIA), about 0.35 ka BP, already identified by [Hoffmann *et al.*, 2001], the GRIP deuterium excess shows two major drops during the Holocene: about 8.2 ka BP and about 4.5 ka BP. The two time periods where GRIP and NorthGRIP  $\delta^{18}\text{O}$  behave differently are also clearly recorded in GRIP deuterium excess and should correspond to dramatic changes in GRIP moisture source evaporation conditions. Unexpectedly, NorthGRIP deuterium excess does not mimic GRIP deuterium excess. During these three events, NorthGRIP exhibits either a small deuterium excess increases (8.2 ka BP), in phase opposition to GRIP deuterium excess decreases, or no clear signal.

[26] The quantitative site and source temperature reconstruction (Figure 2b) suggests that NorthGRIP and GRIP moisture sources undergo significant centennial temperature decreases during the LIA ( $-1^\circ\text{C}$  in Greenland,  $-2^\circ\text{C}$  at GRIP moisture source) and at 8200 BP ( $-1^\circ\text{C}$  for NorthGRIP,  $-2^\circ\text{C}$  at GRIP moisture source,  $-2.5^\circ\text{C}$  for GRIP site). This order of magnitude for Summit temperature change during the 8.2 ka BP event is still significantly smaller than firn gas isotope temperature reconstructions (from 5.4 to 11.7°C estimated by Leuenberger *et al.* [1999]). However, Figure 4, showing individual measurements and reconstructions for the 8200 BP event, points out an intense GRIP cooling ( $-4^\circ\text{C}$ ) during about 25 years (6 samples).

[27] The GRIP and NorthGRIP site temperature reconstructions also exhibit a “medieval warm period” occurring prior to the last millennium, consistently with climate records of high northern latitudes [Bradley *et al.*, 2003]. These events do not clearly imprint on the NorthGRIP moisture source (small signal of opposite sign), again suggesting that GRIP receives a larger proportion of its moisture from higher latitudes undergoing similar climatic changes as central Greenland, whereas NorthGRIP receives a slightly larger proportion of moisture from remote sources (Figure 5).

[28] A cooling of the north Atlantic area results in both a large cooling of the moisture source and a cooling of Greenland temperatures, resulting in a GRIP excess drop and a partial compensation inducing a relatively stable  $\delta^{18}\text{O}$  in the GRIP ice core. This scenario is possible for the 8200 BP and LIA events. Finally, the 4500 BP cooling strongly imprinted in GRIP site and source temperatures could be related to processes affecting local cyclogenesis, for instance in the Labrador Sea [Krinner *et al.*, 1997]. Ocean sediment cores from Baffin Bay [Levac *et al.*, 2001],

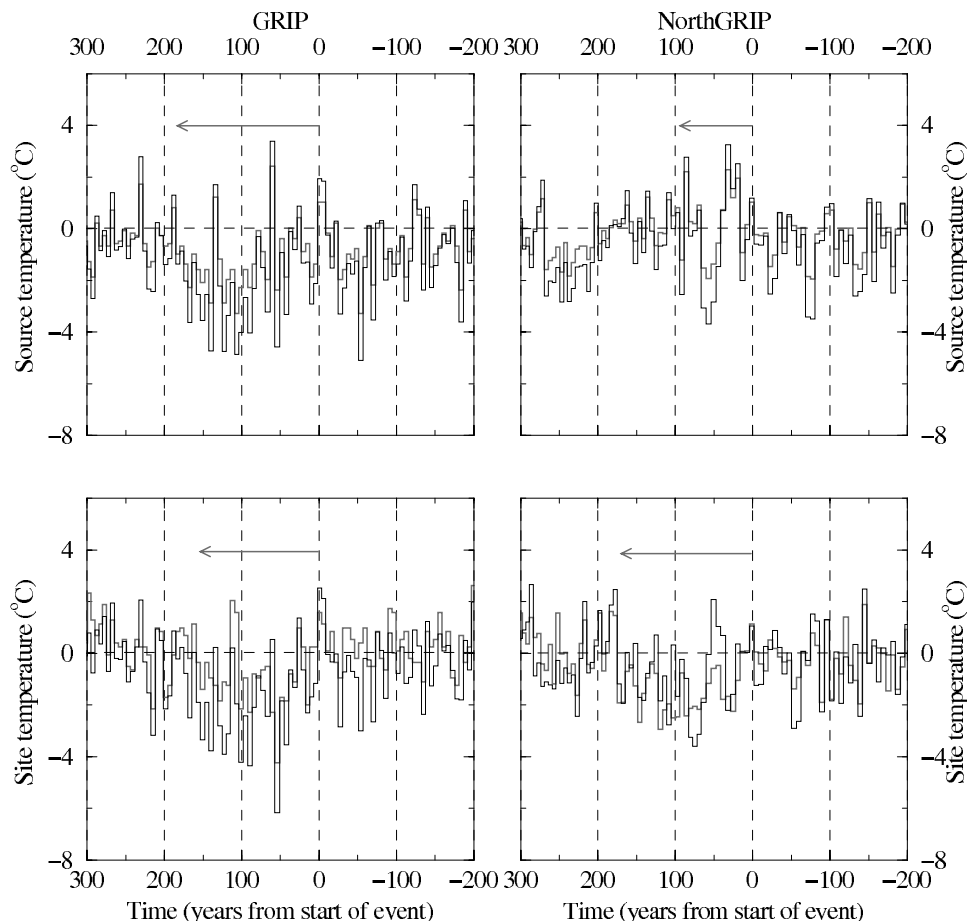


**Figure 4.** Variations of site and source temperatures during the 8.2 kBP event. (left) GRIP. (right) NorthGRIP. (top) Source temperature (black is from our reconstruction, and red is from a  $1^{\circ}\text{C}$  per ‰ conversion from the deuterium excess only). (bottom) Site temperature (black is from our reconstruction, and red is from the spatial slope of  $0.67\text{‰}$  per  $^{\circ}\text{C}$  conversion directly using the  $\delta^{18}\text{O}$  profiles). The timescale is centered on the start of the event (the last positive temperature anomaly before the prolonged cooling episode). The arrows indicate estimates of the event duration. See color version of this figure at back of this issue.

the East Greenland Shelf [Jennings *et al.*, 2001], as well as northern Greenland driftwood occurrence [Bennike, 2004] indeed suggest an increase in sea ice extent during the last 3 to 5 millennia.

[29] NorthGRIP isotopic data suggest a moisture source rather unaffected by the 8.2, 4.5 and LIA events. In this respect, NorthGRIP  $\delta^{18}\text{O}$  would be a better temperature proxy (because only weakly affected by moisture source changes) and GRIP deuterium excess would be a marker of high-latitude source conditions. The shape of the GRIP source temperature decreases during the 8200 BP, 4500 BP and LIA events shows each time a rapid decrease followed by a progressive return to normal levels. Moreover, the sign of GRIP excess anomalies (always negative) clearly point out to radically different rapid event properties during the Holocene compared to rapid events during the last glacial period. Indeed, rapid events of the last glacial period appear as abrupt deuterium excess maxima associated with each Greenland temperature minima [Landais *et al.*, 2004a; Masson-Delmotte *et al.*, 2005; J. Jouzel *et al.*, Rapid deuterium-excess changes in Greenland ice cores: A link between

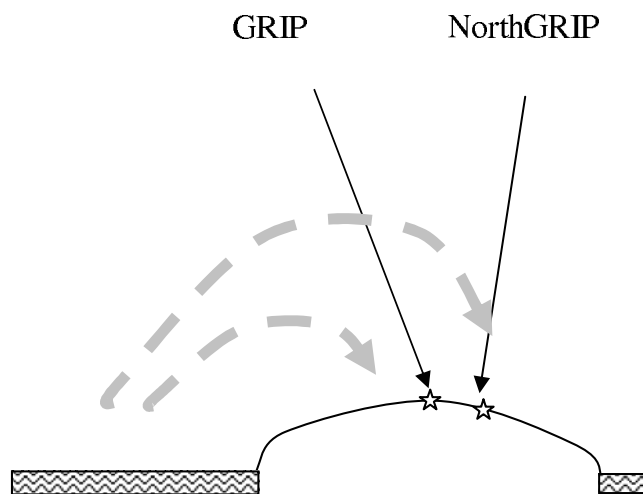


**Figure 5.** Schematic view of latitudinal changes in site and source temperature for two moisture sources and Greenland temperature.

**Table 1.** Mid-Holocene Change in Isotopic Interannual Variability as Calculated From 4-Year Time Step Isotopic and Temperature Profiles From GRIP and NorthGRIP<sup>a</sup>

	GRIP $\delta^{18}\text{O}$	GRIP Excess	NorthGRIP $\delta^{18}\text{O}$	NorthGRIP Excess
Control period (last millennium) standard deviation	0.59	0.66	0.60	0.56
Mid-Holocene period (5500 to 6500 BP) standard deviation	0.48	0.71	0.55	0.75
Standard deviation change (mid-Holocene minus control)	-0.11	+0.05	-0.05	+0.19
Mean change (mid-Holocene minus control)	+0.43	-0.07	+0.58	+0.06

<sup>a</sup>Unit is per mil.

the ocean and the atmosphere (in French with English abstract), submitted to *Comptes Rendus Géosciences*, 2005].

[30] In addition to the centennial-scale fluctuations, the GRIP and NorthGRIP isotopic records discussed here sample high-frequency climate variability. In order to estimate the Holocene changes of this variability, we have calculated a running standard deviation using a 4 year time step for  $\delta^{18}\text{O}$ , deuterium excess, as well as estimated site and source temperatures (not shown) and extracted the results for two time periods: (1) the last 1000 years and (2) from 5500 to 6500 years ago (Table 1). We have verified that the effect of removing the long-term trends does not impact the main conclusions, which however are subject to smoothing due to isotopic diffusion. The same conclusions are reached from the initial isotopic profiles and from the reconstructed site and source temperatures. The interannual variability is largest at the beginning of the Holocene (before 8000 years ago), followed by a minimum about 7000 years ago. It therefore seems that the warmest temperature conditions are associated with a larger interannual stability. There is a  $\sim 20\%$  increasing trend in the  $\delta^{18}\text{O}$  interannual variability during the past 7000 years at both GRIP and NorthGRIP, and a  $\sim 25\%$  decreasing trend of the excess interannual variability during the past 6000 years. We therefore suggest that the interannual variability is inversely related to the mean climate state, with warm conditions systematically associated with a larger stability and a decreased interannual variability.

[31] This diagnostic can similarly be extracted from climate model simulations and therefore should enable to evaluate the realism of the simulated variability of such coupled ocean-atmosphere-sea-ice models. For reference, we have displayed in Table 1 the mean isotopic levels and standard deviation for the last millennium and the millennium centered at 6000 years ago. Intercomparisons of long control simulations performed with such models clearly point to large systematic differences in the spectrum of simulated variability, and capturing correctly this variability is critical with respect to the validity of future climate change forecasts.

## 5. Conclusions

[32] Located about 320 km apart, GRIP and NorthGRIP deep ice cores record different climate histories in their isotopic composition of the ice with regional differences in moisture advection which vary with time. We have shown that they may have slightly different moisture origin nowadays, which needs to be checked with backtrajectories, mesoscale atmospheric models equipped with explicit moisture tagging and/or isotopic modeling.

[33] We suggest that GRIP Holocene  $\delta^{18}\text{O}$  record is more strongly affected by compensation effects between site and source temperature co-fluctuations than NorthGRIP, which receives a larger proportion of its moisture from remote sources. Site and source compensation effects have to be taken into account even during the Holocene, as in Antarctica [Masson-Delmotte *et al.*, 2004].

[34] GRIP and NorthGRIP deuterium excess records show systematic Holocene-long increasing trends, which can be related to changes in the obliquity of the Earth as for Antarctica. The progressive Holocene decrease in obliquity results in an increase of low-latitude annual mean insolation (a warming of low-latitude ocean temperatures), a decrease of high-latitude annual mean insolation (a cooling of high-latitude oceans), and an increase in the latitudinal temperature gradient, which should enhance the relative contribution of (relatively warmer) low latitudes to the Greenland moisture supply and provides a consistent explanation for the observed deuterium excess increase.

[35] We suggest that the GRIP deuterium excess is a better record of north Atlantic hydrological cycle reorganizations. When quantified in terms of GRIP source temperature, it reveals three events with abrupt temperature decreases of  $\sim 2^\circ\text{C}$  followed by a progressive return to normal conditions, 8200, 4500 and  $\sim 350$  years ago. The first event is believed to reflect a change in north Atlantic thermohaline circulation in response to the last massive freshwater input from the Laurentide area. The last event could be related to the Little Ice Age and the Maunder minimum of solar activity, possibly amplified by atmospheric circulation changes in the north Atlantic sector. The 4500 BP event is not so clearly recorded at other locations and could be specific to GRIP and the most local moisture source region (such as the Labrador Sea).

[36] In addition changes in the seasonality of the precipitation may take place during the Holocene, in response for instance to orbital forcing. Coupled ocean-atmosphere simulations forced by mid-Holocene insolation could bring insights on the seasonality induced biases, if the midlatitude atmospheric stationary waves reveal significant changes as suggested by [Masson *et al.*, 1998].

[37] The so-called 8.2 ka BP rapid event is clearly recorded in the  $\delta^{18}\text{O}$  profiles of the GRIP and NorthGRIP deep ice cores. This rapid event has however a very specific but small imprint on the deuterium excess profiles: (1) It is only visible in GRIP deuterium excess signal, suggesting that it significantly affects only the GRIP and not North GRIP moisture source (limited geographical spread) and (2) it is recorded as a GRIP deuterium excess abrupt decrease, while all the other cold events during the glacial period are associated with a deuterium excess increase, reflecting probably drastic changes in the evaporation

areas. We therefore suggest that the 8.2 ka rapid event does differ from the rapid climatic events recorded in full glacial conditions. Whether this behavior is common or not to other rapid events taking place during periods of intermediate extent of the ice sheets could be evaluated by detailed studies conducted on the first rapid event (Dansgaard-Oeschger 25) recorded during this climatic cycle in North-GRIP  $\delta^{18}\text{O}$  [North Greenland Ice Core Project Members, 2004]. Last, the high-resolution isotopic records also enable us to estimate the changes in interannual variability associated with the mean changes and can be compared with transient simulations conducted with climate models.

## Appendix A: Isotopic Modeling

[38] We used here the Mixed Cloud isotopic model (MCIM) developed by *Ciais and Jouzel* [1994] to simulate Antarctic isotopic processes and applied to take into account deuterium excess fluctuations on Antarctic temperature reconstructions [e.g., *Cuffey and Vimeux*, 2001; *Stenni et al.*, 2001].

[39] This distillation model includes parameterizations for key aspects of cloud physics in the line of cloud isotopic models developed by *Fisher* [1990] and *Johnsen et al.* [1989] and more recently *Kavanaugh and Cuffey* [2003]. During evaporation at the ocean surface, the diffusion coefficients for the different molecules had been determined by *Merlivat* [1978] and new estimates have been provided by *Cappa et al.* [2003] leading to relative imprint of diffusion transport on  $\delta\text{D}$  and  $\delta^{18}\text{O}$ . Such a difference on diffusion coefficients has a potential significant influence on the final snow isotopic composition. We have therefore used two versions of the MCIM with different kinetics and included the results in the model sensitivity analyses.

[40] Temperature thresholds determine the onset of ice crystals formation and the final freezing of supercooled liquid are fixed, with Bergeron-Findeisen process affecting the clouds being a mixture of liquid and solid water between these thresholds. As previously demonstrated by *Ciais and Jouzel* [1994], the parameterization of this mixed zone (temperature thresholds, proportion of ice crystal relative to liquid droplets) will not infer strongly on the isotopic composition of the falling snow and its relation to temperature. Indeed, the snow isotopic composition is mostly controlled by the relative values of the solid-vapor equilibrium and kinetic fractionation coefficients at the temperature of condensation. In order to represent correctly the spatial distribution of deuterium excess the cloud temperature threshold for the first crystal formation is fixed to  $-5^\circ\text{C}$ ; most of ice crystals condensate at cloud temperatures of about  $-10^\circ\text{C}$ . This temperature may change with changes in cloud condensation nuclei but on the basis of *Bory et al.* [2003], however, Greenland ice core dust is formed of illite and kaolite usually associated with ice crystal formation at  $-9^\circ\text{C}$ .

[41] While the equilibrium coefficients are well known from experiments and spectroscopic data, the expression of the kinetic fractionation associated to the ice crystal growth is more uncertain. It combines the relative value of diffusion coefficient of the different water molecules in the air and the value of supersaturation over ice during crystal growth. Supersaturation is usually parameterized with a linear rela-

tionship to temperature ( $S = a - bT$ , with  $a$  of the order of 1 and  $b$  a few  $10^{-3}$ ). This function was tuned to represent correctly spatial deuterium excess fluctuations in Antarctica [*Kavanaugh and Cuffey*, 2003; *Petit et al.*, 1991]. The spatial variability of deuterium excess in Greenland is much less constrained (Figure 3) and we used the same expression for supersaturation as for Antarctica with a reasonable agreement with available Greenland surface data. We used two different supersaturation functions depending on the evaporation kinetic parameterization chosen ( $S_{\text{cappa}} = 1.00 - 0.0030T$ ,  $S_{\text{merlivat}} = 1.02 - 0.0038T$ ) to fit the polar transects of both poles. With these two different parameterizations and tunings for the MCIM, sensitivity experiments conducted to very similar results concerning the relative influences of  $T_{\text{source}}$  and  $T_{\text{site}}$  on  $\delta^{18}\text{O}$  and  $d$ , strengthening the validity of the proposed temperature inversion.

[42] The isotopic simulations are also particularly sensitive to the prescribed the proportion of condensates which precipitate out of the clouds (controlling the closed cloud versus open cloud distillation, and therefore related to the relative weight of clear-sky snowfall with respect to the local cyclonic activity). This latter coefficient requires to be specifically increased for a reasonable simulation of central Greenland modern isotopic levels, by contrast to the usual model tuning for Antarctic conditions. Adjusting the cloud microphysics makes sense when considering that clear-sky precipitation plays a much larger role in central Antarctica than in central Greenland, where most snowfall is due to storm tracks. Another assumption concerns the vertical temperature profile, linking surface to condensation temperatures. We use here the same rough assumption as for central Antarctica, i.e., a linear dependency of condensation temperature to surface temperature. *Krinner et al.* [1997] suggested that changes in vertical temperature profiles were rather limited in central Greenland even between glacial and modern conditions. However, we are aware that the vertical atmospheric structure should be less stable in central Greenland than in Antarctica, which could be explored using atmospheric reanalyses (H. Sodemann, personal communication, 2004).

[43] We have performed simulations forced with the observed annual mean latitudinal distribution of sea surface conditions (temperatures, relative humidity, wind speed) to evaluate the isotopic dependency on different source conditions. The model tuning used here is consistent with modern moisture source temperatures ranging from  $15$  to  $20^\circ\text{C}$ ; different MCIM tunings could be obtained with slightly colder moisture source temperatures but with the same model sensitivity [*Johnsen et al.*, 1989]. Indeed, sensitivity studies conducted with varying site and source temperatures allow us to estimate the dependency of central Greenland stable isotopes, all other parameters being fixed. The uncertainties on the slope arise from changing from the Cappa to the Merlivat diffusions and by using different tunings of the supersaturation and precipitation fallout coefficients.

$$\Delta\delta^{18}\text{O} = (0.85 \pm 0.06)\Delta T_{\text{site}} - (0.51 \pm 0.05)\Delta T_{\text{source}} \quad (\text{A1})$$

$$\Delta d = (-0.20 \pm 0.10)\Delta T_{\text{site}} + (0.71 \pm 0.07)\Delta T_{\text{source}} \quad (\text{A2})$$



[44] These coefficients have been obtained within a range of glacial-interglacial temperature variations (about 25°C for site temperature range and 10°C for source temperature range).  $\delta^{18}\text{O}$  and excess have to be corrected for seawater isotopic composition (by  $-0.96\text{‰}$  per ‰ for  $\delta^{18}\text{O}$  and  $+2.1\text{‰}$  per ‰ for deuterium excess) (see Jouzel *et al.* [2003] for the exact analytical calculation). The relative imprint of site and source temperature on each isotope is rather robust with respect to the adjustment of the MCIM, within typically 20%. An inversion of these equations leads to

$$\Delta T_{\text{site}} = (1.32 \pm 0.10)\Delta\delta^{18}\text{O}_{\text{corr}} + (1.04 \pm 0.12)(\Delta d_{\text{corr}} \pm 0.30) \quad (\text{A3})$$

$$\Delta T_{\text{source}} = (0.29 \pm 0.15)\Delta\delta^{18}\text{O}_{\text{corr}} + (1.58 \pm 0.12)(\Delta d_{\text{corr}} \pm 0.30) \quad (\text{A4})$$

[45] The latter result is obtained assuming no other effects control the relationship between precipitation stable isotopes and climatic parameters. The error bar on the reconstructed site and source temperature is estimated from the uncertainty on these regressions together with the uncertainty on the mean deuterium excess measurements (on a 25 year time step we estimate the analytical uncertainty to be  $\pm 0.3\text{‰}$ ); the analytical uncertainty on  $\delta^{18}\text{O}$  can be neglected). Typical uncertainties of 0.5°C for site temperature and 1°C for source temperature are obtained with this calculation. They do not account for non linear changes in surface versus condensation temperatures or in relative humidity versus source temperature, which we cannot estimate with the available information.

[46] This simple isotopic modeling approach offers a framework in which the observed isotopic fluctuations can be quantified and specifically the relative imprint of changes in source versus site temperatures on  $\delta^{18}\text{O}$  and deuterium excess. However, this crude approach does not integrate the changes in central Greenland vertical temperature profile, moisture source wind speed, relative humidity at the moisture source, or changes in air mass history and trajectory, which we know are probably important even at the inter-annual scale (when NAO type of variability has to be considered).

[47] **Acknowledgments.** The  $\delta\text{D}$  analyses were performed at LSCE with support from CEA and from CNRS (Programme National d'Etude Du Climat, IMPAIRS). The isotopic work previously performed by H.F. at the Institute for Environmental Physics, University of Heidelberg, has been funded by "Deutsche Forschungsgemeinschaft" (Wa709/2). We thank G. Hoffmann, U. von Grafenstein, F. Vimeux, and G. Schmidt for sharing ideas and suggestions to improve this paper. We also thank the two anonymous reviewers for their suggestions.

## References

- Alley, R. B., P. A. Mayewski, T. Sowers, M. Stuiver, K. C. Taylor, and P. U. Clark (1997), Holocene climatic instability: A large, widespread event 8200 years ago, *Geology*, *25*, 483–486.
- Andersen, C., N. Koç, A. Jennings, and J. T. Andrews (2004), Nonuniform response of the major surface currents in the Nordic Seas to insolation forcing: Implications for the Holocene climate variability, *Paleoceanography*, *19*, PA2003, doi:10.1029/2002PA000873.
- Appenzeller, C., T. F. Stocker, and M. Anklin (1998), North Atlantic Oscillation dynamics recorded in Greenland ice cores, *Science*, *282*, 446–449.
- Barber, D. C., A. Dyke, C. Hillaire-Marcel, A. E. Jennings, J. T. Andrews, M. W. Kerwin, G. Bilodeau, R. McNeely, J. Southon, and M. D. Morehead (1999), Forcing of the cold event of 8,200 years ago by catastrophic drainage of Laurentide lakes, *Nature*, *400*, 344–347.
- Barlow, L. K., J. W. C. White, R. G. Barry, J. C. Rogers, and P. M. Grootes (1993), The North Atlantic Oscillation signature in deuterium and deuterium excess signals in the Greenland ice sheet project 2 ice core, 1840–1970, *Geophys. Res. Lett.*, *20*(24), 2901–2904.
- Bennike, O. (2004), Holocene sea-ice variations in Greenland: Onshore evidence, *Holocene*, *14*, 607–613.
- Berger, A. (1978), Long-term variation of daily insolation and Quaternary climatic changes, *J. Atmos. Sci.*, *35*(12), 2362–2367.
- Bianchi, G. G., and I. N. M. Cave (1999), Holocene periodicity in North Atlantic climate and deep-ocean flow south of Iceland, *Nature*, *397*, 515–517.
- Bond, G., W. Showers, M. Cheseby, R. Lotti, P. Almasi, P. deMonacal, P. Priore, H. Cullen, I. Hadjas, and G. Bonani (1997), A pervasive millennial-scale cycle in North Atlantic Holocene and glacial climates, *Science*, *278*, 1257–1266.
- Bory, A. J.-M., P. E. Biscaye, A. M. Piotrowski, and J. P. Steffensen (2003), Regional variability of ice core dust composition and provenance in Greenland, *Geochem. Geophys. Geosyst.*, *4*(12), 1107, doi:10.1029/2003GC000627.
- Braconnot, P., O. Marti, S. Joussaume, and Y. Leclainche (2000), Ocean feedback in response to 6 kyr BP insolation, *J. Clim.*, *13*, 1537–1553.
- Bradley, R., M. K. Hughes, and H. F. Diaz (2003), Climate in medieval time, *Science*, *302*, 404–405.
- Bromwich, D. H., R. I. Cullather, and Q.-S. Chen (1998), Evaluation of recent precipitation studies for Greenland ice sheet, *J. Geophys. Res.*, *103*(D20), 26,007–26,024.
- Bromwich, D. H., Q. S. Chen, Y. F. Li, and R. I. Cullather (1999), Precipitation over Greenland and its relation to the North Atlantic Oscillation, *J. Geophys. Res.*, *104*(D18), 22,103–22,115.
- Cappa, C. D., M. B. Hendricks, D. J. DePaolo, and R. C. Cohen (2003), Isotopic fractionation of water during evaporation, *J. Geophys. Res.*, *108*(D16), 4525, doi:10.1029/2003JD003597.
- Ciais, P., and J. Jouzel (1994), Deuterium and oxygen 18 in precipitation: An isotopic model including mixed cloud processes, *J. Geophys. Res.*, *99*(D8), 16,793–16,803.
- Craig, H., and L. I. Gordon (1965), Deuterium and oxygen 18 variations in the ocean and the marine atmosphere, in *Stable Isotopes in Oceanographic Studies and Paleotemperatures*, pp. 9–130, Cons. Naz. delle Ric., Lab. di Geol. Nucl., Pisa, Italy.
- Cuffey, K. M., and F. Vimeux (2001), Covariation of carbon dioxide and temperature from the Vostok ice core after deuterium-excess correction, *Nature*, *412*, 523–527.
- Cuffey, K. M., G. D. Clow, R. B. Alley, M. Stuiver, E. D. Waddington, and R. W. Saltus (1995), Large Arctic temperature change at the Wisconsin-Holocene glacial transition, *Science*, *270*, 455–458.
- Dahl-Jensen, D., N. Gundestrup, K. Keller, S. J. Johnsen, S. P. Gogineni, C. T. Allen, T. S. Chuah, H. Miller, S. Kipfstuhl, and E. D. Waddington (1997), A search in north Greenland for a new ice-core drill site, *J. Glaciol.*, *43*, 300–306.
- Dahl-Jensen, D., K. Mosegaard, N. Gundestrup, G. D. Clow, S. J. Johnsen, A. W. Hansen, and N. Balling (1998), Past temperatures directly from the Greenland ice sheet, *Science*, *282*, 268–271.
- Dansgaard, W. (1964), Stable isotopes in precipitation, *Tellus*, *16*, 436–468.
- Dansgaard, W., S. J. Johnsen, H. B. Clausen, D. Dahl-Jensen, N. S. Gundestrup, C. U. Hammer, J. P. Steffensen, A. Sveinbjörnsdottir, J. Jouzel, and G. Bond (1993), Evidence for general instability of past climate from a 250-kyr ice-core record, *Nature*, *364*, 218–220.
- Fawcett, P. J., A. M. Agustdottir, R. B. Alley, and C. A. Shuman (1995), Change in seasonality in central Greenland across the younger Dryas–preboreal climate transition arising from a poleward shift in winter storm tracks, *Eos Trans. AGU*, *76*, 177.
- Fischer, H., D. Wagenbach, M. Laternser, and W. Häberli (1995), Glaciometeorological and isotopic studies along the EGIG line, central Greenland, *J. Glaciol.*, *41*, 515–527.
- Fischer, H., M. Werner, D. Wagenbach, M. Schwager, T. Thorsteinsson, F. Wilhelms, S. Kipfstuhl, and S. Sommer (1998), Little Ice Age clearly recorded in northern Greenland ice cores, *Geophys. Res. Lett.*, *25*(10), 1749–1752.
- Fisher, D. A. (1990), A zonally averaged stable-isotope model coupled to a regional variable elevation stable isotope model, *Ann. Glaciol.*, *14*, 65–72.
- Fisher, D. A., R. M. Koerner, and N. Reeh (1995), Holocene climatic records from Agassiz Ice Cap, Ellesmere Island, NWT, Canada, *Holocene*, *5*, 19–41.



- Gasse, F., and E. Van Campo (1994), Abrupt post-glacial events in west Asia and north Africa, *Earth Planet. Sci. Lett.*, *126*, 453–456.
- Grafenstein, U. V., E. Erlenkeuser, J. Müller, J. Jouzel, and S. Johnsen (1998), The cold event 8200 years ago documented in oxygen isotope records of precipitation in Europe and Greenland, *Clim. Dyn.*, *14*, 73–81.
- Hoffmann, G., M. Stievenard, J. Jouzel, J. W. C. White, and S. J. Johnsen (1998), Deuterium excess record from central Greenland, modelling and observations, in *Isotope Techniques in the Study of Environmental Changes*, pp. 591–602, Int. At. Energy Agency, Vienna.
- Hoffmann, G., J. Jouzel, and S. J. Johnsen (2001), Deuterium excess record from central Greenland over the last millennium: Hints of a North Atlantic signal during the Little Ice Age, *J. Geophys. Res.*, *106*(D13), 14,265–14,274.
- Houghton, J. T. (Ed.) (2001), *Climate Change 2001: The Scientific Basis*, 896 pp., Cambridge Univ. Press, New York.
- Jennings, A. E., K. L. Knudsen, M. Hald, C. V. Hansen, and J. T. Andrews (2001), A mid-Holocene shift in Arctic sea-ice variability on the East Greenland Shelf, *Holocene*, *12*, 49–58.
- Johnsen, S., W. Dansgaard, and J. White (1989), The origin of Arctic precipitation under present and glacial conditions, *Tellus, Ser. B*, *41*, 452–468.
- Johnsen, S., D. Dahl-Jensen, N. Gundestrup, J. P. Steffensen, H. B. Clausen, H. Miller, V. Masson-Delmotte, A. E. Sveinbjörnsdóttir, and J. White (2001), Oxygen isotope and palaeotemperature records from six Greenland ice-core stations: Camp Century, Dye-3, GRIP, GISP2, Renland and NorthGRIP, *J. Quat. Sci.*, *16*, 299–307.
- Jouzel, J., and L. Merlivat (1984), Deuterium and oxygen 18 in precipitation: Modeling of the isotopic effects during snow formation, *J. Geophys. Res.*, *89*(D7), 11,749–11,757.
- Jouzel, J., et al. (1997), Validity of the temperature reconstruction from ice cores, *J. Geophys. Res.*, *102*(C12), 26,471–26,487.
- Jouzel, J., F. Vimeux, N. Caillon, G. Delaygue, G. Hoffmann, V. Masson-Delmotte, and F. Parrenin (2003), Magnitude of the isotope/temperature scaling for interpretation of central Antarctic ice cores, *J. Geophys. Res.*, *108*(D12), 4361, doi:10.1029/2002JD002677.
- Kavanaugh, J. L., and K. M. Cuffey (2003), Space and time variation of  $\delta^{18}\text{O}$  and  $\delta\text{D}$  in Antarctic precipitation revisited, *Global Biogeochem. Cycles*, *17*(1), 1017, doi:10.1029/2002GB001910.
- Krinner, G., C. Genthon, and J. Jouzel (1997), GCM analysis of local influences on ice core delta signals, *Geophys. Res. Lett.*, *24*(22), 2825–2828.
- Landais, A., J. M. Barnola, V. Masson-Delmotte, J. Jouzel, J. Chappellaz, N. Caillon, C. Hubert, M. Leuenberger, and S. Johnsen (2004a), A continuous record of temperature evolution over a whole sequence of Dansgaard-Oeschger events during Marine Isotopic Stage 4 (76 to 62 kyr BP), *Geophys. Res. Lett.*, *31*, L22211, doi:10.1029/2004GL021193.
- Landais, A., N. Caillon, A. Grachev, J. M. Barnola, J. Chappellaz, J. Jouzel, V. Masson-Delmotte, and M. Leuenberger (2004b), Quantification of rapid temperature change during DO event 12 and phasing with methane inferred from air isotopic measurements, *Earth Planet. Sci. Lett.*, *225*, 221–232.
- Lauritzen, S. E. (2003), Reconstruction Holocene climate records from speleothems, in *Global Change in the Holocene*, edited by A. Mackay et al., pp. 242–263, Edward Arnold, London.
- Leuenberger, M., C. Lang, and J. Schwander (1999), Delta  $^{15}\text{N}$  measurements as a calibration tool for the paleothermometer and gas-ice age differences: A case study for the 8200 B.P. event on GRIP ice, *J. Geophys. Res.*, *104*(D18), 22,163–22,170.
- Levac, E., A. D. Vernal, and W. Blake (2001), Sea surface conditions in the northernmost Baffin Bay during the Holocene: Palynological evidence, *J. Quat. Sci.*, *16*, 353–363.
- Liu, Z., E. Brady, and J. Lynch-Stieglitz (2003), Global ocean response to orbital forcing in the Holocene, *Paleoceanography*, *18*(2), 1041, doi:10.1029/2002PA000819.
- Marchal, O., et al. (2002), Apparent long-term cooling of the sea surface in the northeast Atlantic and Mediterranean during the Holocene, *Quat. Sci. Rev.*, *21*, 455–483.
- Masson, V., S. Joussaume, S. Pinot, and G. Ramstein (1998), Impact of parameterizations on simulated winter mid-Holocene and last glacial maximum climatic changes in the Northern Hemisphere, *J. Geophys. Res.*, *103*(8), 8935–8943.
- Masson, V., R. Cheddadi, P. Braconnot, S. Joussaume, and D. Texier (1999), Mid-Holocene climate in Europe: What can we infer from PMIP model-data comparisons, *Clim. Dyn.*, *15*, 163–182.
- Masson-Delmotte, V., B. Stenni, and J. Jouzel (2004), Common millennial scale variability of Antarctic and southern ocean temperatures during the past 5000 years reconstructed from EPICA dome C ice core, *Holocene*, *14*, 145–151.
- Masson-Delmotte, V., J. Jouzel, A. Landais, M. Stievenard, S. J. Johnsen, J. W. C. White, A. Sveinbjörnsdóttir, K. Fuhrer, and E. Cortijo (2005), Deuterium excess reveals millennial and orbital scale fluctuations of Greenland moisture origin, *Science*, in press.
- McDermott, F., D. P. Matthey, and C. Hawkesworth (2001), Centennial-scale Holocene climate variability revealed by a high-resolution speleothem delta O-18 record from SW Ireland, *Science*, *294*, 1328–1331.
- Merlivat, L. (1978), The dependence of bulk evaporation coefficients on air-water interfacial conditions as determined by the isotopic method, *J. Geophys. Res.*, *83*(C6), 2977–2980.
- Merlivat, L., and J. Jouzel (1979), Global climatic interpretation of the deuterium-oxygen 18 relationship for precipitation, *J. Geophys. Res.*, *84*(C8), 5029–5033.
- North Greenland Ice Core Project Members (2004), High resolution climate record of the Northern Hemisphere reaching into last interglacial period, *Nature*, *431*, 147–151.
- O'Brien, S. R., P. A. Mayewski, L. D. Meeker, D. A. Meese, M. S. Twickler, and S. I. Whitlow (1995), Complexity of Holocene climate as reconstructed from a Greenland ice core, *Science*, *270*, 1962–1964.
- Petit, J. R., J. W. C. White, N. W. Young, J. Jouzel, and Y. S. Korotkevich (1991), Deuterium excess in recent Antarctic snow, *J. Geophys. Res.*, *96*(D3), 5113–5122.
- Renssen, H., H. Goosse, T. Fichefet, V. Brovkin, E. Driesschaert, and F. Wolk (2005), Simulating the Holocene climate evolution at northern high latitudes using a coupled atmosphere-sea ice-ocean-vegetation model, *Clim. Dyn.*, *24*, 23–43.
- Rimbu, N., G. Lohmann, J.-H. Kim, H. W. Arz, and R. Schneider (2003), Arctic/North Atlantic Oscillation signature in Holocene sea surface temperature trends as obtained from alkenone data, *Geophys. Res. Lett.*, *30*(6), 1280, doi:10.1029/2002GL016570.
- Rozanski, K., L. Araguas-Araguas, and R. Gonfiantini (1993), Isotopic patterns in modern global precipitation, in *Climate Change in Continental Isotopic Records*, *Geophys. Monogr. Ser.*, vol. 78, edited by P. K. Swart et al., pp. 1–37, AGU, Washington, D. C.
- Rühlemann, C., S. Mulitza, P. J. Müller, G. Wefer, and R. Zahn (1999), Warming of the tropical Atlantic Ocean and slowdown of thermohaline circulation during the last deglaciation, *Nature*, *402*, 511–514.
- Severinghaus, J. P., and E. Brook (1999), Simultaneous tropical-Arctic abrupt climate change at the end of the last glacial period inferred from trapped air in polar ice, *Science*, *286*, 930–934.
- Severinghaus, J. P., T. Sowers, E. Brook, R. B. Alley, and M. L. Bender (1998), Timing of abrupt climate change at the end of the younger Dryas interval from thermally fractionated gases in polar ice, *Nature*, *391*, 141–146.
- Shindell, D. T., G. A. Schmidt, M. E. Mann, D. Rind, and A. Waple (2001), Solar forcing of regional climate change during the Maunder Minimum, *Science*, *294*, 2149–2152.
- Stenni, B., V. Masson-Delmotte, S. Johnsen, J. Jouzel, A. Longinelli, E. Monnin, R. Roethlisberger, and E. Selmo (2001), An oceanic cold reversal during the last deglaciation, *Science*, *293*, 2074–2077.
- Vimeux, F., V. Masson, J. Jouzel, J. R. Petit, E. J. Steig, M. Stievenard, R. Vaikmae, and J. W. C. White (2001), Holocene hydrological cycle changes in the southern hemisphere documented in East Antarctic deuterium excess records, *Clim. Dyn.*, *17*, 503–513.
- Vinther, B., S. J. Johnsen, K. K. Andersen, H. B. Clausen, and A. W. Hansen (2003), NAO signal recorded in the stable isotopes of Greenland ice cores, *Geophys. Res. Lett.*, *30*(7), 1387, doi:10.1029/2002GL016193.
- Werner, M., U. Mikolajewicz, M. Heimann, and G. Hoffmann (2000), Borehole versus isotope temperatures on Greenland: Seasonality does matter, *Geophys. Res. Lett.*, *27*(5), 723–726.
- Werner, M., M. Heimann, and G. Hoffmann (2001), Isotopic composition and origin of polar precipitation in present and glacial climate simulations, *Tellus, Ser. B*, *53*, 53–71.

O. Cattani, S. Falourd, J. Jouzel, A. Landais, V. Masson-Delmotte, and M. Stievenard, IPSL/CEA, CNRS LSCE, F-91191 Gif-sur-Yvette, France. (masson@lsce.saclay.cea.fr)

D. Dahl-Jensen and S. J. Johnsen, Niels Bohr Institute, University of Copenhagen, DK-2100 Copenhagen, Denmark.

H. Fischer, Alfred Wegener Institute for Polar and Marine Research, D-27515 Bremerhaven, Germany.

T. Popp and J. W. C. White, Geological Sciences Department, University of Colorado, Boulder, CO 80309, USA.

A. Sveinbjörnsdóttir, Science Institute, University of Iceland, Dunhaga 3, IS-101 Reykjavik, Iceland.

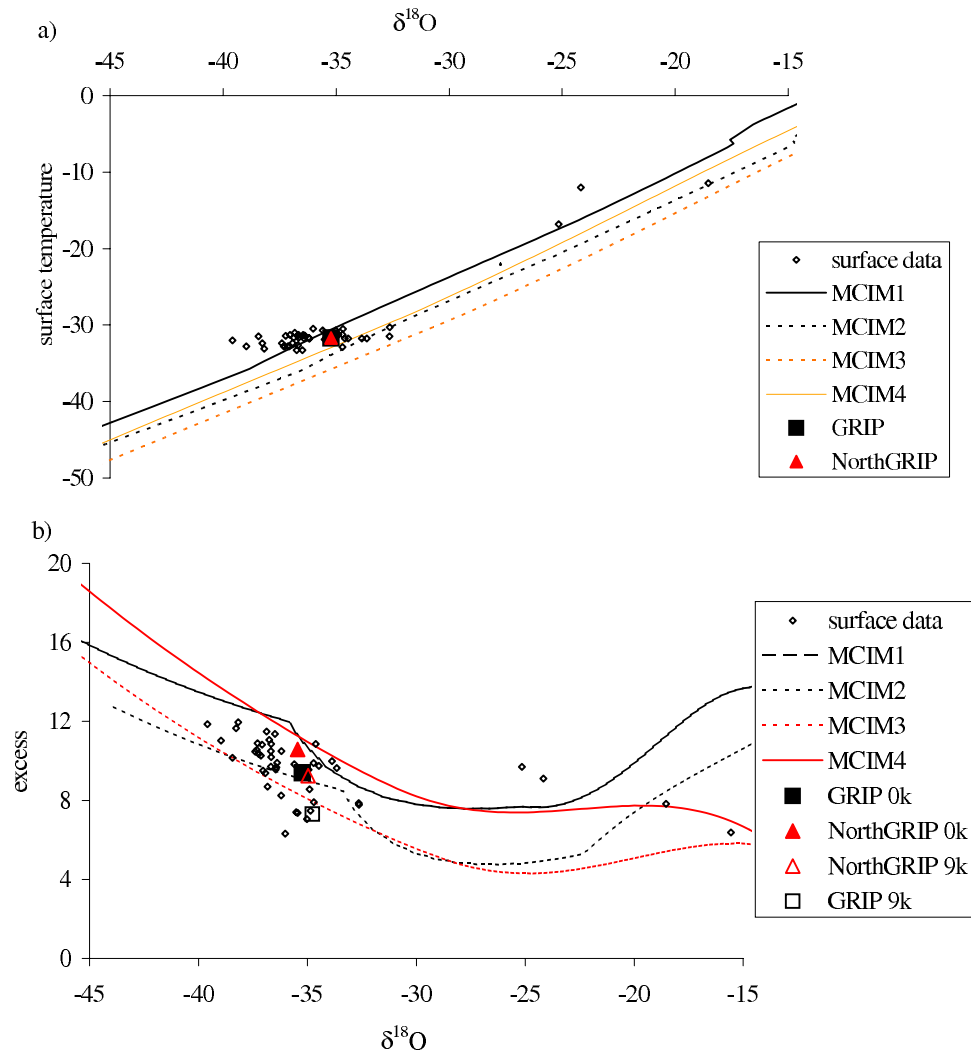


**Figure 3.** (a) The  $\delta^{18}\text{O}$  ( $x$  axis) versus local surface temperature ( $y$  axis). Surface temperatures are either directly available or are estimated from a linear regression on site latitude and elevation, fitted to the 19 direct temperature measurements available among the Greenland sites described in Figure 1a (with slopes of  $7.9^\circ\text{C}$  per 1000 m elevation and a slope of  $1.0^\circ\text{C}$  per degree latitude); long-term mean annual  $\delta^{18}\text{O}$  is estimated from IAEA stations along the duration of monitoring and over the last 50 years from traverse pits (squares) and from GRIP and NorthGRIP (triangles) ice cores. Simulations performed with the MCIM isotopic model with source temperatures of  $15^\circ\text{C}$  (dashed line) and  $20^\circ\text{C}$  (solid line) are also displayed, with two versions of the MCIM (Merlivat coefficients, MCIM1 and 2, and Cappa coefficients, MCIM3 and 4). The model-data disagreement for coastal stations might result from large contribution of local moisture supply with colder source temperatures. (b) Same as Figure 3a but for observed and simulated deuterium excess as a function of  $\delta^{18}\text{O}$ .

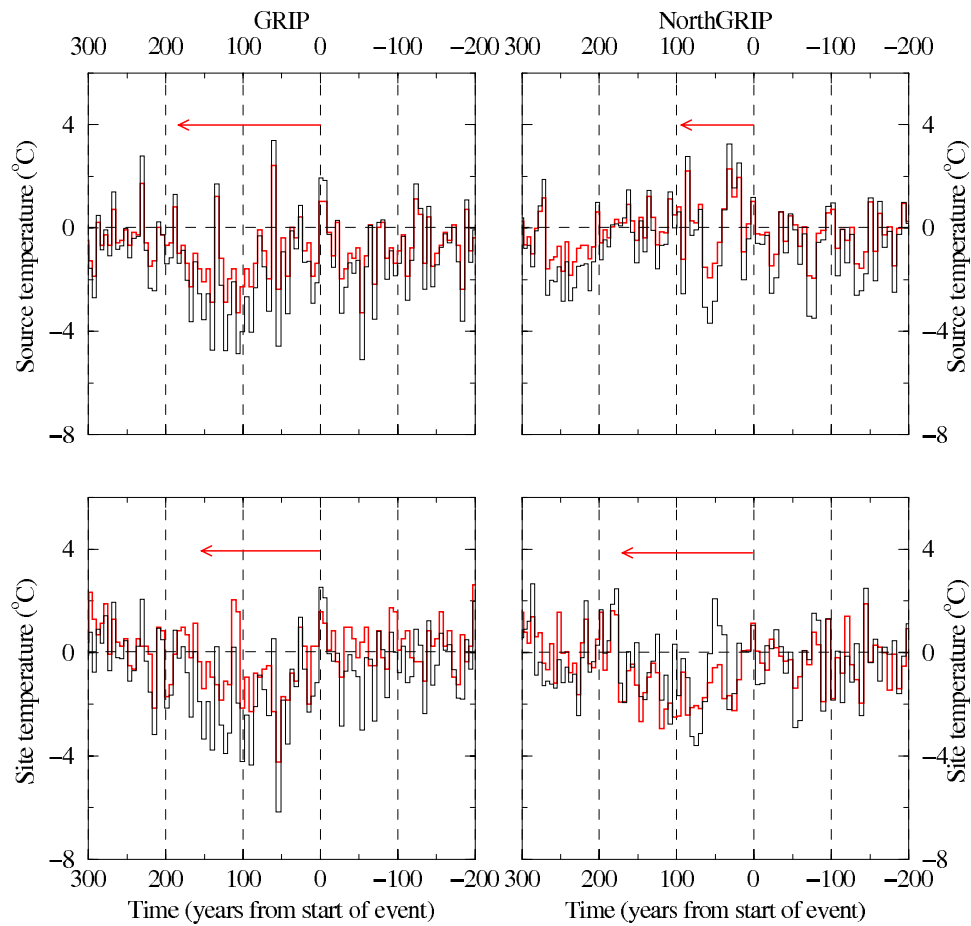


**Figure 4.** Variations of site and source temperatures during the 8.2 kBP event. (left) GRIP. (right) NorthGRIP. (top) Source temperature (black is from our reconstruction, and red is from a  $1^{\circ}\text{C}$  per ‰ conversion from the deuterium excess only). (bottom) Site temperature (black is from our reconstruction, and red is from the spatial slope of  $0.67\text{‰}$  per  $^{\circ}\text{C}$  conversion directly using the  $\delta^{18}\text{O}$  profiles). The timescale is centered on the start of the event (the last positive temperature anomaly before the prolonged cooling episode). The arrows indicate estimates of the event duration.